Journal of Cleaner Production 227 (2019) 88–97

Contents lists available at ScienceDirect

Journal of Cleaner Production

journal homepage: www.elsevier.com/locate/jclepro

Utilizing low-cost natural waste for the removal of pharmaceuticals from water: Mechanisms, isotherms and kinetics at low concentrations

Yuan Li [a, c, *], Mark A. Taggart [a], Craig McKenzie [b], Zulin Zhang [c], Yonglong Lu [d], Sabolc Pap [a, e], Stuart Gibb [a]

[a] Environmental Research Institute, North Highland College, University of the Highlands and Islands, Castle Street, Thurso, Caithness, Scotland, KW14 7JD, UK
[b] Forensic Drug Research Group, Centre for Anatomy and Human Identification, School of Science and Engineering, University of Dundee, Nethergate, Dundee, DD1 4HN, UK
[c] Environmental and Biochemical Sciences Group, James Hutton Institute, Craigiebuckler, Aberdeen, AB15 8QH, UK
[d] Research Centre for Eco-Environmental Sciences, Chinese Academy of Sciences, 18 Shuangqing Road, Haidian District, Beijing, 100085, China
[e] University of Novi Sad, Faculty of Technical Sciences, Department of Environmental Engineering and Occupational Safety and Health, 21000, Novi Sad, Serbia

ARTICLE INFO

Article history:
Received 6 November 2018
Received in revised form
19 February 2019
Accepted 8 April 2019
Available online 11 April 2019

Keywords:
Low-cost waste material
Circular economy
Water remediation
Biosorption mechanisms
Pharmaceuticals
Sustainable development

ABSTRACT

The use of abundant natural wastes as environmentally friendly products promotes a circular green economy and cleaner production. The potential use of natural waste materials without additional processing for the removal of priority pharmaceuticals from water was investigated. Here, the performance of selected low-cost biosorbents (biochar, macro-algae and wood chippings) was evaluated using two extensively prescribed model pharmaceuticals: diclofenac (DCF) and trimethoprim (TMP). The physicochemical properties of the biosorbents were examined (to shed light on likely biosorption mechanisms) using Brunauer–Emmett–Teller (BET) measurements, scanning electron microscopy (SEM), zero point of charge (pH_{zpc}) measurements and Fourier transform infrared spectroscopy (FTIR). Experimental data from kinetic studies fitted a pseudo-second order model, and multiple diffusion steps limited the mass transfer of analytes. Intra-partile diffusion was the rate limiting step for biochar, while macro-algae and wood chippings were limited (mainly) by adsorptive attachment. The equilibrium data for most of the studied systems best fitted a Langmuir model, while the Freundlich model provided a better fit for TMP with wood chippings. At $\mu g \cdot L^{-1}$ initial pharmaceutical loading levels, the maximum biosorption capacity for DCF was attained with biochar ($7.25 \times 10^3\ \mu g\ g^{-1}$), while macro-algae performed best for TMP ($7.14 \times 10^4\ \mu g\ g^{-1}$). Both chemical and physical interactions were likely responsible for the biosorption of pharmaceuticals. High removal efficiencies were achieved at the low initial loadings studied, indicating the potential application of those sustainable low-cost biosorbents at low (environmentally relevant) pharmaceutical concentrations.

1. Introduction

With a growing and aging population, and with improving living standards and health care provision in many regions of the world, the use of human pharmaceuticals is increasing. Worldwide, prescribed medication costs were US$996 billion in 2017 (Statista, 2017). The presence of pharmaceuticals in natural waters is now well documented and is of growing global concern, e.g. Aaus der Beek et al. (2016) reported that >600 pharmaceuticals have been detected in the environment from 71 countries. These chemicals are not only present at quantifiable levels in urban and industrial regions but also in rural areas with low population density and low industrial intensity (Nebot et al., 2015). There are significant concerns that pharmaceuticals in the environment are linked to the development of (multi-) resistant bacterial strains, and, that non-target eco-

* Corresponding author. Environmental Research Institute, Castle Street, Thurso, Scotland, KW14 7JD, UK.
E-mail address: Yuan.Li2@uhi.ac.uk (Y. Li).

https://doi.org/10.1016/j.jclepro.2019.04.081
0959-6526/

toxicological effects on wild organisms may occur (Carlsson et al., 2013; Kuzmanović et al., 2015; Weigmann, 2017). For instance, diclofenac has caused the virtual extinction of certain vulture species across much of Asia (Oaks et al., 2004), trimethoprim has been found to inhibit the growth of freshwater microalgae (De Liguoro et al., 2012), fluoxetine has been shown to cause reproductive delay in leopard frogs (Foster et al., 2010), and ciprofloxacin has proven to be genotoxic to aquatic bacteria and to reduce algal diversity (Wilson et al., 2003). These effects have led to a desire to better remove such compounds from aqueous media, however, conventional treatment processes applied in wastewater treatment plants (WWTPs) are often not sufficient to remove all pharmaceutical residues (Rivera-Utrilla et al., 2013). Therefore, novel, effective and sustainable solutions are required to eliminate pharmaceutical residues before their introduction into the aquatic environment.

In addressing this challenge, sorption processes may have certain advantages in terms of effectiveness, simplicity, low cost and sustainability (Rivera-Utrilla et al., 2013; Wang and Wang, 2016). Activated carbons (ACs) are undoubtedly one of the most widely studied sorbent materials which could/are being applied in water treatment (Yu et al., 2016), however, application is often restricted by high manufacturing costs (700–5000 US$/ton) (Mailler et al., 2016). Alternatively, biosorbents can turn waste agro- and/or industrial by-products into low-cost resources for water remediation and support the principles of the circular economy. Various materials have been explored for the removal of dyes and heavy metals, and recently, some have been trialled for pharmaceutical elimination. However, most work has involved extra modification or a synthesis process (Ali et al., 2018; Żółtowska-Aksamitowska et al., 2018). The evaluation of low-cost materials derived from agro- and/or industrial wastes (without additional functionalization) for the removal of pharmaceutical residues, especially at relatively low concentrations, is still limited.

Diclofenac (DCF) is a non-steroidal anti-inflammatory drug (NSAID) used to treat pain and reduce inflammation, which is extensively used worldwide and has been found in effluents from WWTPs at concentrations of 2.3–510 $\mu g\,L^{-1}$ and in surface waters up to 500 $ng\,L^{-1}$ (Ashton et al., 2004; Bu et al., 2013; Kasprzyk-Hordern et al., 2009). It has now been added to the European Priority Watch List of the Environmental Quality Standards Directive and is classified as a highly persistent substance by the Stockholm County Council (Barbosa et al., 2016; Directive, 2015/495; Mailler et al., 2016). Trimethoprim (TMP) is a widely prescribed antibiotic, which is also used as a veterinary antibiotic (2.9 tons in the UK in 2000), and has been reported as the most frequently occurring antibiotic found in UK wastewaters (up to 1300 $ng\,L^{-1}$) (Ji et al., 2016; Regulation, 37/2010). It is of concern as a persistent emerging contaminant and has been monitored in veterinary practice by EU (Regulation, 37/2010; Sarmah et al., 2006). Despite their being no limits for concentrations of pharmaceuticals in water after treatment, the legislation has driven the water industry to monitor such chemicals and further control the discharge.

As such, the objective of this study was to evaluate the performance of three low-cost biosorbents (biochar, macro-algae and wood chippings) for the removal of two priority pharmaceuticals (DCF and TMP) from aqueous media at low concentrations ($\mu g \cdot L^{-1}$) by assessing (1) impact factors, (2) the kinetics of the intra-particle diffusion and reaction processes, (3) sorption isotherms, and (4) pH impact and interaction mechanisms.

2. Materials and methods

2.1. Chemicals

DCF and TMP were obtained as high purity reference standards (HPLC-grade, ⩾97%) from Sigma Aldrich. Acetonitrile, formic acid and ammonia hydroxide were HPLC grade (Fisher Scientific UK Ltd). The physico-chemical properties of DCF and TMP are shown in Table S1.

2.2. Biosorbents

In preliminary studies, eleven materials from agricultural and industrial wastes (as listed in Supporting Information Table S2) were processed and screened for their ability to remove pharmaceuticals from a test solution. From these, the three most efficient biosorbents were chosen for further investigation in this study: a biochar, macro-algae (brown seaweed, *Fucus vesiculosus*), and oak wood chippings.

The biochar was produced in a pyrolysis plant using orchard pruning residues (garden wastes) combusted at 500 °C and has an organic matter content of ~50% (Beesley et al., 2013). This biochar was selected as that with the best performance in the preliminary studies (data not shown) from a number of biochars derived from various sources. The macro-algae was harvested from local beaches near Thurso (UK), and the wood chippings were collected from oak tree waste from Aberdeen (UK). Each material was ground using a food processor (Binifnett KH 525) and sieved. The 0.25–0.8 mm fraction was the particle size used for all the biosorbents in this study. Materials were washed with methanol and Milli-Q water separately (three times) and dried at 105 °C until constant mass.

2.3. Physical characterisation

Textural characterisation was carried out using N_2 sorption/desorption isotherms through Brunauer-Emmett-Teller (BET) analysis. The specific surface area and pore structure parameters of the biosorbents were evaluated. The surface morphology of biosorbents was studied by Scanning Electron Microscopy (SEM; Topcon SM-300 SEM). Potentiometric titration procedures were performed to investigate the zero point of charge (pH_{zpc}) using methods reported by Faria et al. (2004). Fourier transform infrared spectroscopy (FTIR) was conducted using a Nicolet Magna-IR 550 FTIR spectrometer (Thermo Electron, Warwick, UK) to elucidate the characteristic functional groups present on the biosorbents before and after biosorption.

2.4. Analyte quantification

The concentration of pharmacueticals in water samples was determinated by high performance liquid chromatography tandem mass spectrometry (LC-MS/MS) using an Alliance 2695 HPLC (Waters; Manchester, UK) coupled to a Micromass® Quattro Micro™ MS detector with electrospray ionisation (ESI). A Phenomenex Kinetic EVO C18 5 μm 4.6 × 100 mm column and negative ESI mode was used for DCF determination, while TMP determination used a Waters X Bridge C18 2.5 μm 2.1 × 100 mm column and positive ESI mode. The elution gradient programs are summarized in Table S3. For the MS/MS detection, two transitions were monitored for each compound for quantification and qualification (for DCF: 294 > 250, 214; for TMP: 291 > 230, 261). The limits of detection (LOD; signal-to-noise of 3) for DCF and TMP were 0.4 and 0.05 $\mu g\,L^{-1}$, respectively.

To correct for instrumental drift/sensitivity fluctuations, an external standard of 500 $\mu g\,L^{-1}$ was injected between each series of samples (n = 12). Concentrations were calculated with respect to an eight-point calibration curve (2–500 $\mu g\,L^{-1}$). Data analysis was conducted using Masslynx™ NT software (Waters; Milford, MA, USA).

2.5. Biosorption experiments

All experiments were conducted as batch studies, in triplicate. To approach the biosorption behaviour of pharmaceuticals in real environmental conditions, the pH of the solution was adjusted to pH 7 using 0.1 M NaOH/HCl prior to the biosorption experiments, except where the effect of pH was being investigated. A detailed description is given below, where C_0 is the initial concentration of model pharmaceuticals, pH is the initial pH of the aqueous phase, m is the mass of the biosorbent used, V is the volume of the aqueous phase and t is the contact time.

(i) Effect of initial biosorbent loading (dosage impact): $C_0 = 500\ \mu g\ L^{-1}$; $m = 1–40\ g\ L^{-1}$; $V = 25$ mL; pH = 7; $t = 0–24$ h
(ii) Effect of contact time (kinetics): $C_0 = 500\ \mu g\ L^{-1}$; $m = 0.5\ g\ L^{-1}$ (DCF-biochar), $20\ g\ L^{-1}$ (DCF-others), $2\ g\ L^{-1}$ (TMP); $V = 100$ mL; pH = 7; $t = 0–24$ h
(iii) Effect of initial pharmaceutical concentration (isotherms): $C_0 = 100–20{,}000\ \mu g\ L^{-1}$ (DCF) and $100–400{,}000\ \mu g\ L^{-1}$ (TMP); $m = 0.5\ g\ L^{-1}$ (DCF-biochar), $20\ g\ L^{-1}$ (DCF-others), $2\ g\ L^{-1}$ (TMP); $V = 50$ mL; pH = 7; $t = 24$ h
(iv) Effect of initial solution pH: $C_0 = 500\ \mu g\ L^{-1}$; $m = 0.5\ g\ L^{-1}$ (DCF-biochar), $20\ g\ L^{-1}$ (DCF-others), $2\ g\ L^{-1}$ (TMP); $V = 25$ mL; pH = 3, 5, 7, 9, 11; $t = 24$ h

During the biosorption experiments, samples were taken at predetermined time intervals using 2 mL luer lock plastic syringes (NORM-JECT®) and filtered with 0.2 μm PTFE (polytetrafluoroethylene) disposable syringe filtration membranes (Fisher Scientific). The experiments were conducted at 20 °C on a flat-bed shaker (300 rpm).

The uptake of pharmaceuticals ($\mu g \cdot g^{-1}$) was quantified based on the following mass balance equation:

$$Q = \frac{(C_0 - C_t)V}{m} \quad (1)$$

where Q ($\mu g \cdot g^{-1}$) is the amount of adsorbate sorbed, C_0 and C_t ($\mu g \cdot L^{-1}$) are the pharmaceutical concentration at initial ($t = 0$ h) and at time t, respectively, V (mL) is the volume of the aqueous phase and m (g) is the mass of the biosorbent. The kinetic and isotherm equilibrium models used to fit data are presented in Table S4.

3. Results and discussion

3.1. Characterisation of biosorbents

The biosorbent textural properties were evaluated by BET. The highest surface area and total pore volume were found for biochar, at $8.89\ m^2\ g^{-1}$ and $1.86 \times 10^{-2}\ cm^3\ g^{-1}$, respectively, followed by wood chippings ($1.77\ m^2\ g^{-1}$ and $3.81 \times 10^{-3}\ cm^3\ g^{-1}$) and macro-algae ($0.29\ m^2\ g^{-1}$ and $6.47 \times 10^{-4}\ cm^3\ g^{-1}$). The average pore diameter of the biochar was 20.11 Å while that of wood chippings and macro-algae was around 16.35 Å. Taking the molecular diameters for DCF (7.7 Å) and TMP (8.1 Å) into consideration, the pores present in these biosorbents potentially allow pharmaceuticals to enter. The pore-filling process may be particularly favourable in biochar due to its higher pore volume and average pore diameter. Fig. S1 shows SEM images of the biosorbents at 500 × and 3000 × magnification. The morphologies of the biosorbents were predominantly irregular in shape with the biochar demonstrating greater internal porosity than the macro-algae and wood chippings (as seen at 3000 × magnification). This was in agreement with the BET analysis.

The plot to determine pH_{zpc} for the biosorbents is shown in Fig. S2. The intersection of the curve representing pH_{final} versus $pH_{initial}$ occurred at 9.1 for biochar (which corresponds to the point of zero charge) showing the basic character of this material. For macro-algae and wood chippings, pH_{final} values increased with increasing $pH_{initial}$ up to pH 5 then remained nearly constant up to pH 10, which can be attributed to the change in surface charge from positive to negative. The pH_{zpc} was 5.5 for macro-algae and 5.7 for wood chippings.

FTIR spectra (Fig. S3) were recorded in the range of $400–4000\ cm^{-1}$ to examine the functional groups present on the biosorbents both before and after biosorption of DCF and TMP, and therefore, help identify the groups participating in the biosorption process. We observed that the vibrational bands in the biochar and biochar + adsorbate samples were similar, as shown in Fig. S3a. The sorption band ~$3325\ cm^{-1}$ is assigned to vibration of the hydroxyl groups (O–H) of alcohols, phenols and carboxylic acids in biochar (Artz et al., 2008); $2920\ cm^{-1}$ and $2845\ cm^{-1}$ are attributed to the symmetric and asymmetric stretching vibrations of the C–H bonds of CH_x groups; while $1794\ cm^{-1}$ and $870\ cm^{-1}$ are ascribed to the vibration of carbonate. The band at $1700\ cm^{-1}$ is attributed to stretching vibrations of the C=O bonds of the carboxylic acid group (COOH) and the peak at $1550\ cm^{-1}$ is due to the vibration of aromatic amines (N–H). The bonds at $1415\ cm^{-1}$ and $1030\ cm^{-1}$ are assigned to C–O stretching (Pezoti et al., 2014).

In addition to the identification of the surface properties of the biosorbents, FTIR also confirmed changes in functional groups before and after adsorption. In Fig. S3b, the band at $3265\ cm^{-1}$ is assigned to stretching vibration of hydroxyl groups (O–H) in the raw macro-algae spectrum, and this is shifted to $3310\ cm^{-1}$ after biosorption for both DCF and TMP, indicating that some interaction bonds are formed during biosorption between hydroxyl groups in macro-algae and the pharmaceutical molecules. The major groups found in macro-algae also include, aliphatic C–H ($2922\ cm^{-1}$) and lipids ($2851\ cm^{-1}$), C=O in carboxylic acids ($1710\ cm^{-1}$), N–H (aromatics), C–O in aliphatic esters ($1030\ cm^{-1}$), and proteins ($1613\ cm^{-1}$). For the wood chippings (Fig. S3c), characteristic bands were observed at $3340\ cm^{-1}$ (O–H), $2900\ cm^{-1}$ (C–H of lipids), $1730\ cm^{-1}$ (C=O of acids groups) and $1030\ cm^{-1}$ (C–O of ether groups). The presence of lignocellulose is inferred by the characteristic broad band in the range $1100–1600\ cm^{-1}$ (Sampathkumar et al., 2014).

3.2. Impact of biosorbent dose and contact time

The amount of pharmaceutical sorbed was related to biosorbent dose, i.e., removal efficiency of DCF and TMP from the test solution increased as the biosorbent dose increased (from 1 to 10 or $10–40\ g\ L^{-1}$ Fig. 1) simply due to the increased number of available biosorption sites.

The results are presented in the range of $10–40\ g\ L^{-1}$ (Fig. 1 b.c) since negligible removal of DCF was obtained at lower pharmaceutical dose ($1–10\ g\ L^{-1}$). The optimal dose of macro-algae and wood chippings for $500\ \mu g\ L^{-1}$ DCF was $20\ g\ L^{-1}$, while $1\ g\ L^{-1}$ of biochar provided efficient removal for DCF (Fig. 1a). The uptake of DCF onto macro-algae (Fig. 1b) was not affected by contact time (up to 120min), indicating that active surface sites were limited and those present were occupied rapidly. Interestingly, no clear difference was observed in removal efficiency for macro-algae above the $20\ g\ L^{-1}$ dose, suggesting the limitation of macro-algae biosorption capabilities in short time period. This may be attributed to the competition of the active sites with any organic matters released by macro-algae or any saturation of outer interface coverage of drug molecules occurred onto the macro-algae surface. In the case of the other materials, increased dose and contact time increased DCF

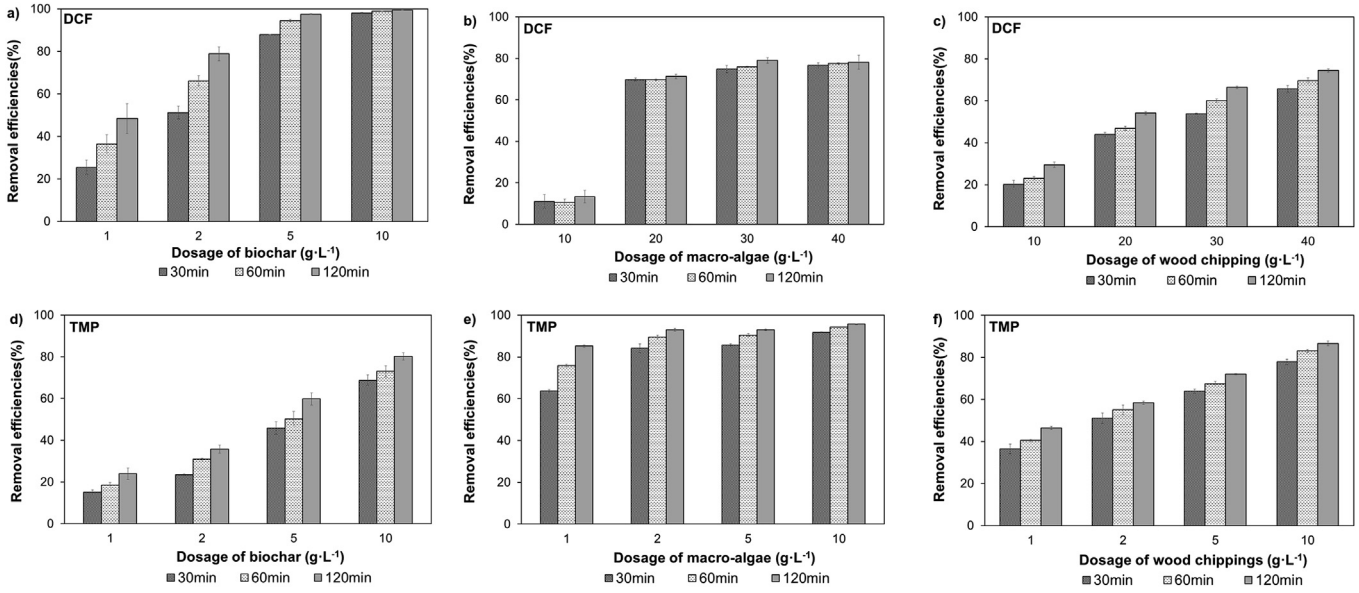

Fig. 1. Biosorbent dose and its impact on sorption of - DCF onto (a) biochar (b) macro-algae (c) wood chippings, and - TMP onto (d) biochar (e) macro-algae (f) wood chippings ($C_0 = 500\ \mu g\ L^{-1}$, $T = 20\ ^\circ C$, pH = 7, $V = 25$ mL, $m = 1, 2, 5, 10, 20, 30, 40\ g\ L^{-1}$, $t = 30, 60, 120$ min).

removal efficiency, suggesting longer term penetration and biosorption into the sorbent matrix.

The removal of TMP from solution is shown in Fig. 1d-f. Considerable removal of TMP was obtained at $2\ g\ L^{-1}$ for all biosorbents. Removal efficiency improved with both increasing dose and time as active biosorption sites increased and contact time potentially allowed deeper sorption/penetration into the biosorbent. Unlike for DCF (removal efficiencies for macro-algae and wood chippings were ostensibly at their maximum at all doses between 10 and $40\ g\ L^{-1}$ as shown in Fig. 1b,c), the removal of TMP at $10\ g\ L^{-1}$ sorbent dose was >80% and increasing the sorbent dose to $40\ g\ L^{-1}$ had little impact on sorption (e.g., removal efficiencies of TMP on macro-algae enhanced from 94 to 96% at 1 h when dosage increased from $10\ g\ L^{-1}$ to $40\ g\ L^{-1}$). At the lower dosage for macro-algae (i.e., $2\ g\ L^{-1}$), as shown in Fig. 1 e, up to 90% of TMP was sorbed after 1 h, indicating that macro-algae possessed the greatest potential for pharmaceuticals like TMP, which are positively charged at typical environmental pH's (6–8).

3.3. Biosorption kinetics

3.3.1. Reaction kinetics

Kinetics describes the rate of adsorbate uptake at the solid-liquid interface and can be used to help design appropriate biosorption technologies. Fig. 2 shows the experimental data for DCF and TMP, the biosorption was rapid in first 2 h and the sorption efficiency increased further up to 24 h, where it appeared to have reached equilibrium. The kinetic data were examined by three models i.e., pseudo-first, pseudo-second order and Elovich models (Table S4).

The kinetic parameters of DCF and TMP are present in Table 1. The correlation coefficients (R^2) and agreement between the experimental data ($Q_{e,exp}$) and the calculated values ($Q_{e,cal}$) indicates that the sorption of both pharmaceuticals best follows a second order kinetic model for all three biosorbents, i.e., that chemisorption dominates these processes (Shi et al., 2009). The linearized pseudo-second order fitted results for DCF and TMP are also shown in Fig. S4. The presence of second order sorption kinetics is in agreement with other sorption studies regarding

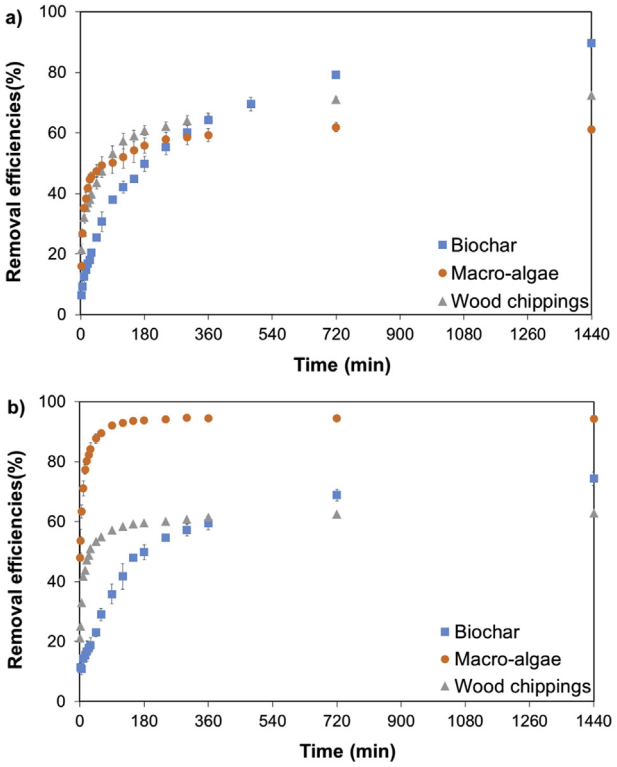

Fig. 2. The biosorption kinetic data for (a) DCF ($m_{biochar} = 0.5\ g\ L^{-1}$ and $m_{others} = 20\ g\ L^{-1}$) and (b) TMP ($m = 2\ g\ L^{-1}$) using biochar, macro-algae and wood chippings ($C_0 = 500\ \mu g\ L^{-1}$, $T = 20\ ^\circ C$, pH = 7, $V = 100$ mL, $t = 0$–1440 min).

pharmaceuticals onto other biosorbents (Bui and Choi, 2009; Larous and Meniai, 2016; Sotelo et al., 2012). The Elovich model (Table S4) takes into account that the solid surface is energetically heterogeneous and that sorption occurs predominantly by chemisorption (Malash and El-Khaiary, 2010). The parameter α therein describes the initial sorption rate (with higher values inferring greater chemisorption), while β is an indicator of desorption. As

Table 1
Biosorption kinetic parameters for DCF and TMP onto three biosorbents.

Biosorbent	Compound	$Q_{e,exp}$ ($\mu g \cdot g^{-1}$)	Pseudo 1st order			Pseudo 2nd order			Elovich		
			$Q_{e,cal}$ ($\mu g \cdot g^{-1}$)	K_1 (min^{-1})	R^2	$Q_{e,cal}$ ($\mu g \cdot g^{-1}$)	K_2 ($g \cdot \mu g^{-1} \cdot min^{-1}$)	R^2	α ($\mu g \cdot g^{-1} \cdot min^{-1}$)	β ($\mu g \cdot g^{-1}$)	R^2
Biochar	DCF	9.89×10^2	16.67	9.21×10^{-4}	0.938	1.01×10^3	6.99×10^{-6}	0.999	3.21×10^1	7.05×10^{-3}	0.962
	TMP	2.20×10^2	8.50	4.61×10^{-4}	0.903	2.22×10^2	3.59×10^{-5}	0.999	1.00×10^1	3.48×10^{-2}	0.953
Macro-algae	DCF	1.53×10^1	7.14	7.14×10^{-3}	0.854	1.55×10^1	4.99×10^{-3}	0.999	3.43×10^1	6.11×10^{-1}	0.928
	TMP	2.38×10^2	5.92	1.93×10^{-2}	0.926	2.38×10^2	1.36×10^{-3}	0.999	9.12×10^5	7.22×10^{-2}	0.783
Wood chippings	DCF	1.81×10^1	2.49	3.69×10^{-3}	0.960	1.83×10^1	2.05×10^{-3}	0.999	9.05	4.53×10^{-1}	0.981
	TMP	1.58×10^2	5.75	1.24×10^{-2}	0.882	1.59×10^2	8.03×10^{-4}	0.999	4.45×10^3	7.73×10^{-2}	0.856

shown in Table 1, low values of β (0.007–0.6 $\mu g\, g^{-1}$) indicate effective interactions between pharmaceuticals and biosorbents, and the irreversibility of these sorption processes. From comparison of values of α (Table 1), it may be inferred that chemisorption of DCF was more significant for biochar and macro-algae than for wood chippings. For TMP, chemisorption was more significant for macro-algae and wood chippings than for biochar. These observations may, in part, explain the removal performances observed (i.e., higher removal efficiency (in Fig. 2) and higher experimental uptake (in Table 1) for macro-algae and wood chippings for TMP than for DCF).

The reaction kinetic model parameters in Table 1 also show that the kinetic constants ($K_{2\ DCF/TMP}$) for macro-algae and wood chippings were considerably higher than for biochar, suggesting that macro-algae and wood chippings reached equilibrium more rapidly. The experimental biochar equilibrium uptake of DCF was much higher than for wood chipping and macro-algae; while the biochar equilibrium uptake of TMP was slightly lower than that of macro-algae, both of which were higher than for wood chippings. This further indicated that biochar was efficient in the removal of negatively ionised pharmaceuticals (like DCF) while macro-algae was more efficient for the removal of positively ionised compounds (like TMP).

3.3.2. Diffusion models

Diffusion kinetic models are used to describe the mass transfer of analytes to the biosorbents by identifying transport pathways and predicting rate-controlling steps. In general, it is known that the four steps associated with transport processes during biosorption are (Weber Jr, 1984): (1) bulk transport (adsorbate transport in the solution phase - occurring instantaneously after biosorbent is transferred to the adsorbate solution); (2) film diffusion (adsorbate transports from the bulk liquid phase to the biosorbent external surface); (3) intra-particle diffusion (diffusion of adsorbate molecules from the exterior of the biosorbent into pores, along pore-wall surfaces or both); (4) adsorptive attachment - equilibrium phase (adsorbate binds to the active sites of the biosorbent). Transport processes can be evaluated using the intra-particle diffusion rate model, which is given in Eq. (2) below (Weber and Morris, 1963):

$$Q_t = K_p \sqrt{t} + C \tag{2}$$

where Q_t ($\mu g \cdot g^{-1}$) is the amount of adsorbate sorbed at t (min), K_p ($\mu g \cdot g^{-1} \cdot min^{1/2}$) is the intra-particle diffusion model constant and C ($\mu g \cdot g^{-1}$) is a constant associated with the thickness of the boundary layer, where a higher C corresponds to a thicker boundary layer with greater limiting effects. The slope K_p and intercept C of plot Q_t versus $t^{1/2}$ was used to calculate the diffusion constant K_p and the thickness of the boundary layer C. The intra-particle diffusion fitting results are presented in Fig. 3. Multiple linear regions indicated that each biosorption system comprised a number of mechanisms. For both DCF and TMP, the analyte mass transfer to biochar was mainly limited by intra-particle diffusion while for macro-algae and wood chippings, it was mostly controlled by the final adsorptive attachment step.

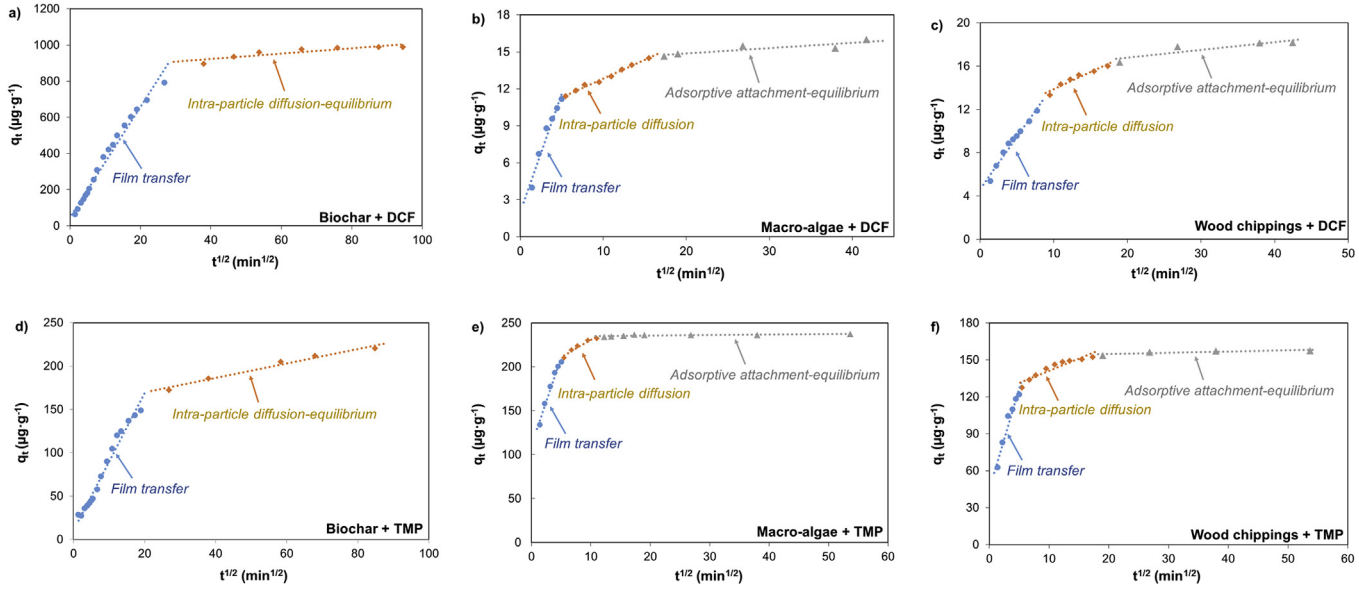

Fig. 3. The intra-particle diffusion of DCF and TMP onto biosorbents.

Table 2
The intra-particle diffusion parameters for DCF and TMP onto three biosorbents.

Biosorbent	Compound	K_{p1} ($\mu g \cdot g^{-1} \cdot min^{-1/2}$)	K_{p2} ($\mu g \cdot g^{-1} \cdot min^{-1/2}$)	K_{p3} ($\mu g \cdot g^{-1} \cdot min^{-1/2}$)	C_1 ($\mu g \cdot g^{-1}$)	C_2 ($\mu g \cdot g^{-1}$)	C_3 ($\mu g \cdot g^{-1}$)	R_1^2	R_2^2	R_3^2
Biochar	DCF	3.06×10^1	1.48	N/A	4.88×10^1	8.64×10^2	N/A	0.980	0.808	N/A
	TMP	7.92	8.38×10^{-1}	N/A	1.04×10^1	1.53×10^2	N/A	0.978	0.976	N/A
Macro-algae	DCF	1.92	3.04×10^{-1}	4.31×10^{-2}	1.99	9.79	1.40×10^1	0.959	0.991	0.762
	TMP	2.00×10^1	3.96	5.97×10^{-2}	1.11×10^2	1.91×10^2	2.34×10^2	0.973	0.938	0.569
Wood chippings	DCF	9.64×10^{-1}	3.18×10^{-1}	7.22×10^{-2}	4.65	1.07×10^1	1.53×10^1	0.972	0.936	0.794
	TMP	1.64×10^1	1.98	9.82×10^{-2}	4.48×10^1	1.21×10^2	1.53×10^2	0.956	0.887	0.731

Table 2 further shows the diffusion parameters (K_p, C) modelled for DCF and TMP with the three biosorbents. The mass transfer of pharmaceuticals to biochar was characterised by both film diffusion (C_1) and intra-particle diffusion (C_2) (e.g., for DCF to biochar, C_2 8.64×10^2 $\mu g\ g^{-1}$ was > C_1 4.88×10 $\mu g\ g^{-1}$). The higher value of C_2 indicated a thicker boundary layer in relation to intra-particle diffusion, and intra-particle diffusion was the rate limiting step for biochar. This result was in accordance with the BET (and SEM) characterisation results presented above. The biochar had a larger surface area (8.89 $m^2\ g^{-1}$) with more interior pores (Fig. S1), which in-turn reduced the rate at which pharmaceuticals reached potential biosorption sites (especially interior sites). We postulate that once the adsorbates are transported to the active sites in the interior pores, attachment occurs quickly. According to the $t^{1/2}$ axis, it can be concluded that it takes longer for biochar (lower slope) in the film diffusion step (compared to macro-algae and wood chippings), which can be attributed to its larger surface area. As the film and intra-particle diffusion steps are much slower, there are only two diffusion steps (linear regions) observed for biochar in the tested time range.

In the case of macro-algae and wood chippings, all these diffusion steps – film, intra-particle diffusion and adsorptive attachment were involved in limiting mass transfer of pharmaceuticals (Fig. 3b,c,e,f). Here, both the film and intra-particle diffusion steps of analytes to macro-algae and wood chippings occurred more quickly (higher slope compared to biochar), which can be attributed to their lower surface areas and total pore volumes. The highest boundary layer referred to the adsorptive attachment step (C_3) for both DCF and TMP (e.g., for DCF to macro-algae: C_3 1.40×10^1 $\mu g\ g^{-1}$ > C_2 9.79 $\mu g\ g^{-1}$ > C_1 1.99 $\mu g\ g^{-1}$). We postulate that the limited interior pores and pore-wall surface become saturated with adsorbate, obstructing adsorptive attachment between the analyte and the active sites, where the analytes would compete for the limited active sites for the final adsorptive attachment. These findings were also in agreement with the characterisation results (BET and Fig. S1). When comparing the results for the two studied pharmaceuticals, the diffusion of DCF into/onto macro-algae and wood chippings was notably quicker than for TMP ($C_{3DCF} < C_{3TMP}$), while it was easier for TMP to bind to biochar ($C_{2TMP} < C_{2DCF}$).

3.4. Isotherms

Biosorption isotherms reveal the relationship between the equilibrium concentration of the analyte (C_e) and the adsorbent uptake (Q_e), and provide insights into the nature of the biosorption phenomenon. Fig. 4a–f therefore gives the biosorption isotherms for DCF and TMP on biochar, macro-algae and wood chippings. In all cases, increased uptake (Q_e) was observed with increased initial pharmaceutical concentration (C_0; Fig. 4a–f; circles). Moreover, higher removal efficiencies (Fig. 4a–f; triangles) were achieved at the lower initial loadings (C_0), indicating the potential application of these biosorbents at low pharmaceutical concentrations.

Langmuir and Freundlich models (Table S4) were applied to examine the isotherms. The Langmuir model estimates the maximum adsorption capacity based on the assumption of a homogeneous and monolayer coverage of adsorbate onto an identical set of well-defined localized biosorption sites without lateral interaction and steric hindrance between biosorbed molecules (Doğan et al., 2000; Langmuir, 1918; Kyzas et al., 2013). The Freundlich model refers to heterogeneous surfaces and encompasses multi-layer coverage via the exponential distribution of

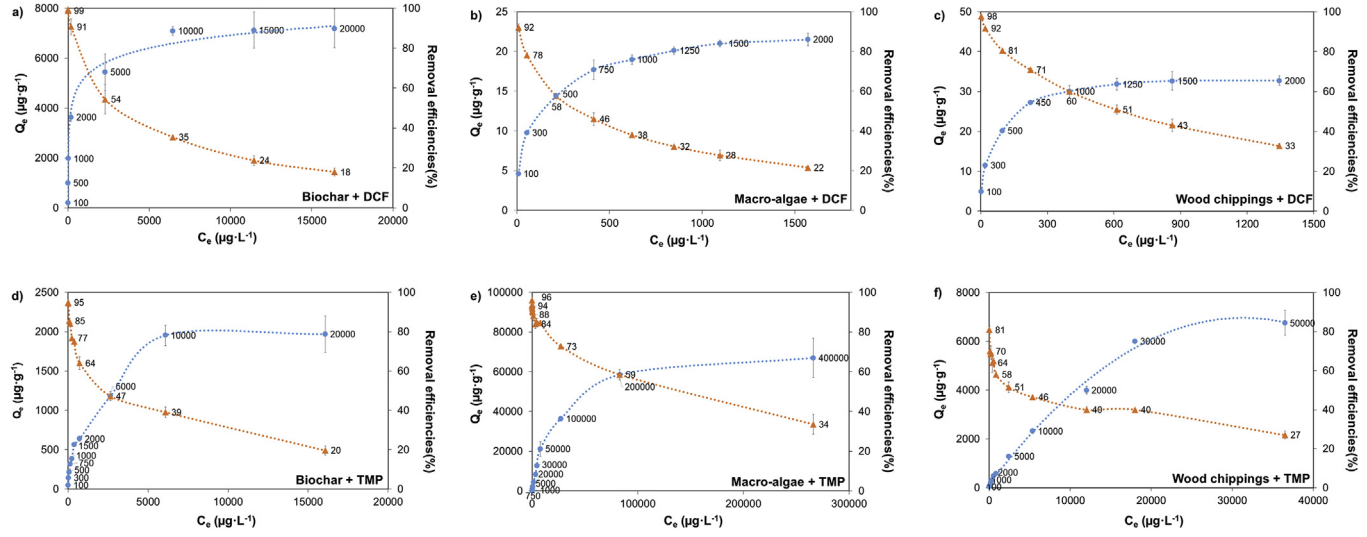

Fig. 4. The biosorption isotherms for DCF sorption onto (a) biochar (0.5 g L^{-1}) (b) macro-algae (20 g L^{-1}) (c) wood chippings (20 g L^{-1}), and TMP onto (d) biochar (e) macro-algae (f) wood chippings (all 2 g L^{-1}) (C_0 = 500 $\mu g\ L^{-1}$, T = 20 °C, pH = 7, V = 50 mL, t = 24 h).

Table 3
Biosorption isotherms parameters for DCF and TMP onto three biosorbents.

Biosorbent	Compound	Langmuir parameters			Freundlich parameters		
		Q_m ($\mu g \cdot g^{-1}$)	K_L ($L \cdot \mu g^{-1}$)	R^2	n	K_F ($\mu g^{1-1/n} L^{1/n} \cdot g^{-1}$)	R^2
Biochar	DCF	7.25×10^3	5.37×10^{-3}	0.998	3.32	5.04×10^2	0.824
	TMP	2.08×10^3	1.17×10^{-3}	0.987	2.18	3.13×10^1	0.974
Macro-algae	DCF	2.24×10^1	1.19×10^{-2}	0.997	3.39	2.76	0.978
	TMP	7.14×10^4	6.66×10^{-5}	0.994	1.42	2.32×10^1	0.979
Wood chippings	DCF	3.38×10^1	2.35×10^{-2}	0.999	3.21	4.29	0.964
	TMP	8.33×10^3	1.10×10^{-4}	0.932	1.41	5.01	0.996

active sites, in which infinite surface coverage is predicted without any saturation onto the biosorbent surface (Freundlich, 1906; Hasley, 1952; Matias et al., 2015).

Table 3 gives the equilibrium parameters for DCF and TMP onto the three biosorbents. The correlation coefficients (R^2) indicated that DCF sorption onto all three sorbents was best represented by the Langmuir model (suggesting monolayer sorption). The sorption capacity for DCF followed the order: biochar (7.25×10^3 $\mu g\, g^{-1}$) > wood chippings (3.38×10^1 $\mu g\, g^{-1}$) > macro-algae (2.24×10^1 $\mu g\, g^{-1}$). For TMP sorption onto biochar, the Langmuir model provided the best fit to the data, while the Freundlich model was better for wood chippings (Table 3). This suggested that the biosorption of TMP onto biochar was predominantly monolayer, while wood chippings involved multi-layer sorption. The biosorption of TMP onto macro-algae fitted both the Langmuir and Freundlich models. This indicated the involvement of both chemical (monolayer) and physical (multi-layer sorption) interactions for macro-algae, which favoured the biosorption of TMP. This hypothesis is validated by the higher maximum biosorption capacity for macro-algae with TMP ($Q_{m\ \text{macro-algae}}$ 7.14×10^4 $\mu g\, g^{-1}$).

In order to compare these low-cost biosorbents with other reported materials, the maximum uptake for DCF and TMP were compared to data from other studies (Table S5.). Excluding the important synthesis costs involved, uptake of DCF here by biochar was not as efficient as for activated carbons (Bhadra et al., 2016, 2017; Sotelo et al., 2014), grape bagasse (Antunes et al., 2012) and organoclays (De Oliveira et al., 2017); but was more efficient than for molecularly imprinted polymer (Madikizela and Chimuka, 2016), sericite hybrid materials (Tiwari et al., 2015), silica-based materials (Bui and Choi, 2009; Suriyanon et al., 2013) and even some carbon nanotubes (Czech and Oleszczuk, 2016). TMP uptake by macro-algae was higher than for a powdered activated carbon (Bonvin et al., 2016), biosorbents derived from sewage sludge (Nielsen and Bandosz, 2016) and montmorillonite (Vidal et al., 2015); but lower than for certain types of activated carbon (Kim et al., 2010; Liu et al., 2012). It should however be noted that a direct comparison between biosorption capabilities is only indicative because of the different experimental conditions used (Kyzas and Deliyanni, 2015). Most studies present their Q_m results obtained at optimum conditions (i.e., the best result from the batch experiments, as shown in Table S5). For instance, the maximum uptake of TMP onto powdered activated carbon was 2.58×10^5 $\mu g\, g^{-1}$ when the initial pH was 4 (Kim et al., 2010); and experiments on mesoporous silica (SBA-15) were conducted in acidic conditions (pH 3–5), which is not applicable to a normal aqueous environment (Bui and Choi, 2009). High pharmaceutical loadings can also contribute to biosorption capabilities (maximising concentration gradients). For example, the Q_m value for grape bagasse was 6.83×10^4 $\mu g\, g^{-1}$, however, removal efficiencies remained at 20% for the 10 mg L^{-1} drug loading in the kinetic work (Antunes et al., 2012). Therefore, the low-cost biosorbents studied here, which performed well with relatively low concentrations of drugs (without extra synthesis costs), may still be promising alternatives for pharmaceuticals removal from aqueous media.

3.5. Effect of pH and interaction mechanisms

pH plays an important role in biosorption as it affects both the surface properties of the biosorbent and the speciation of the analyte. Fig. 5 illustrates the pH effect of biosorption system, expressed in terms of removal efficiencies under different initial pH conditions ($pH\text{-}_{initial}$). For all tested biosorbents, a decrease of pH enhanced the removal of DCF, while the optimal pH conditions for TMP varied.

To evaluate the interaction mechanisms, the charge status of both the biosorbent and analyte, are further depicted in Fig. 6. The surface of a biosorbent is neutral when $pH = pH_{zpc}$, negatively

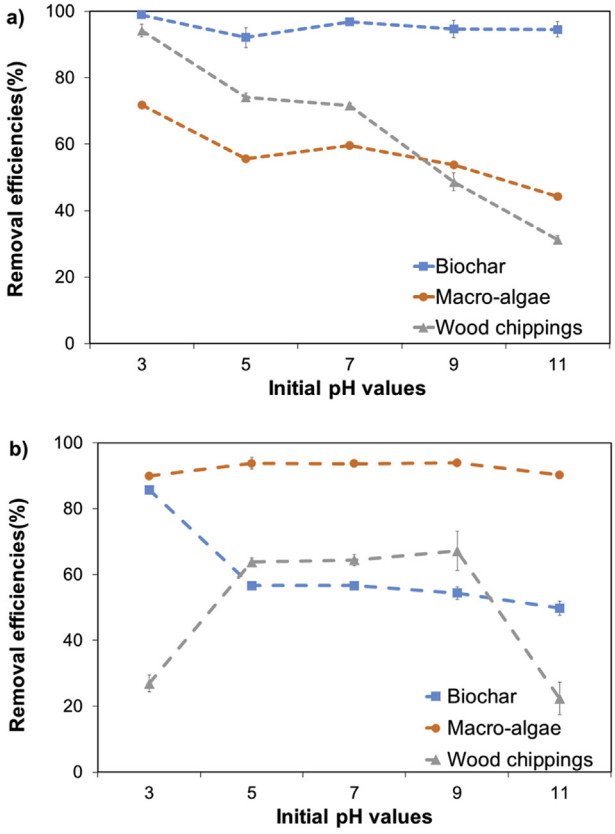

Fig. 5. Removal efficiencies at different initial pH values for (a) DCF ($m_{biochar} = 0.5$ g L^{-1} and $m_{others} = 20$ g L^{-1}) and (b) TMP ($m = 2$ g L^{-1}) ($C_0 = 500$ $\mu g\, L^{-1}$, $T = 20$ °C, pH = 3, 5, 7, 9, 11, $V = 25$ mL, $t = 24$ h).

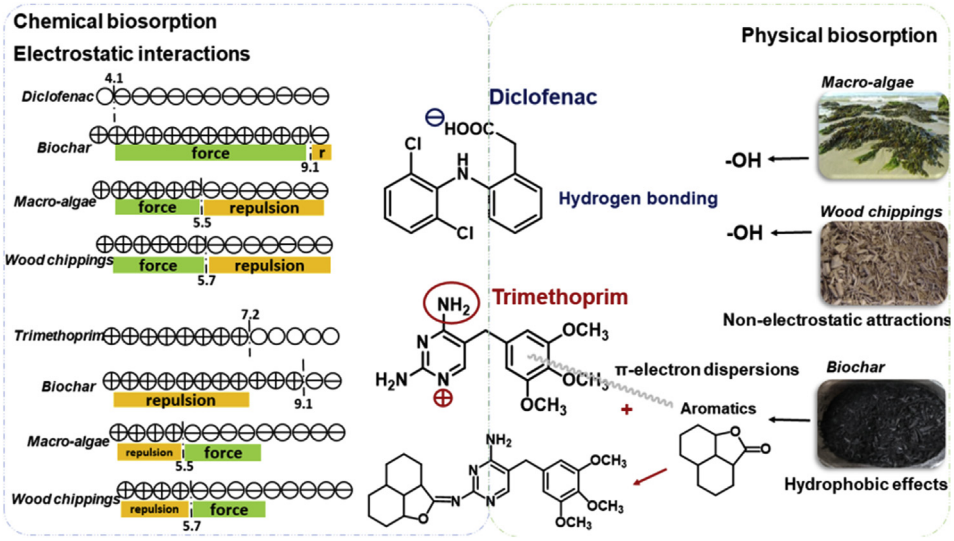

Fig. 6. Biosorption interaction mechanisms for pharmaceuticals onto low-cost biosorbents with surface charge status of biosorbents (pH_{zpc} 9.1; 5.5; 5.7) and protonation–deprotonation status of analytes (pK_a Diclofenac 4.1; Trimethoprim 7.2) Left: hypothesized chemical interactions between ionised pharmaceuticals and charged biosorbents at different pH; Right: postulated physical biosorption mechanisms and proposed interaction between trimethoprim and biochar.

charged for pH's higher than the pH_{zpc}, and positively charged at pH's below the pH_{zpc} (Adriano et al., 2005). In terms of pharmaceuticals, their charge is based on their pK_a value. It should be noted that the addition of the biosorbent can change the pH of the solution, which is defined here as $pH\text{-}_{final}$. The charge status for the biosorbents and analyte at different tested $pH\text{-}_{initial}$, is therefore evaluated by the final pH of the solution (Table S6).

In the case of DCF sorption onto macro-algae, at initial pH 5–7 (pH_{final} ~5), DCF (pK_a 4.1) was predominantly (~90%) present as a negatively charged species and the macro-algae was positively charged ($<pH_{zpc}$ 5.5). Electrostatic interactions are therefore expected to be responsible for the biosorption process. The removal efficiency for DCF by macro-algae then reduced under alkaline conditions ($pH_{initial} = 9$, 11) as electrostatic repulsion was introduced (i.e., DCF and macro-algae both negatively charged as shown in Fig. 6 left). The enhancement of DCF uptake was perceptible at low initial pH (i.e., pH 3), when there was no electrostatic repulsion (a portion of DCF is neutral (pK_a 4.1) and the macro-algae was positively charged ($<pH_{zpc}$ 5.5) – at this point, a physical interaction was involved. This hypothesis was validated by the FTIR results (Fig. S3.), in which the peak of the hydroxyl group (O–H) for macro-algae shifted after biosorption (due to the hydrogen bonding between DCF and macro-algae). As the pH_{zpc} for wood chippings was close to that of macro-algae, similar findings were observed (Fig. 5a.). The proposed interaction mechanisms were depicted in Fig. 6.

In terms of the biosorption of DCF onto biochar, it was noteworthy that the removal efficiencies remained high regardless of pH, which was ascribed to chemical interaction, i.e., electrostatic forces, whereby with pH_{final} between 5 and 9, DCF was negatively charged (pK_a 4.1) and the biochar was positively charged ($<pH_{zpc} = 9.1$). Moreover, physisorption (hydrophobic effects and π-electrons dispersions) may also be involved, as DCF contains both a carboxylate group and two chloro groups, which are electron-acceptors. The electron density in the aromatic rings of the biochar was postulated to be less subject to pH, therefore, DCF was able to continue to have a high affinity for the biochar via π-electron dispersion forces between the π-electrons in DCF and the π-electrons in the aromatics of the biochar. π-electron dispersion interactions have also been reported in other studies involving the biosorption of pharmaceuticals by activated carbon (Baccar et al., 2012).

In terms of TMP, the amino group (–NH–) in the molecule can be positively charged (pK_a 7.2) and uncharged as presented in Fig. 6. Based on data from pH studies (Fig. 5b.), it was evident that the removal efficiency for wood chippings dropped significantly at both more acidic and more alkaline conditions. At initial pH 3 ($pH_{final} = 4$), when both the surface of the wood chippings ($<pH_{zpc}$ 5.7) and TMP ($pK_a = 7.2$) were positively charged, electrostatic repulsion was introduced. In the initial pH range 5–7 ($pH_{final} = 6$), TMP cations were bound to negatively charged wood chippings via electrostatic forces. At initial pH 11 ($pH_{final} = 7$), when a portion of TMP became neutral, TMP molecules were unable to bind to the wood chippings via electrostatic forces. Macro-algae, retained a high affinity to TMP regardless of pH, suggesting interaction was not only due to electrostatic forces (which were only applicable at initial pH 9 ($pH_{final} = 6$). This is also in agreement with the isotherm model results (Langmuir and Freundlich), which suggested both multi-layer (physical) and monolayer (chemical) biosorption interactions were responsible for the process.

In terms of TMP and biochar, electrostatic forces were not at work based on the final pH values, which may help explain why the maximum uptake for biochar was much lower (than for macro-algae and wood chippings). Physisorption, such as pore fillings (as discussed in the characterisation study) may be involved. The acidic pH condition ($pH_{initial} = 3$) favoured the uptake of neutral TMP onto positively charged biochar. At initial pH 5 to 11 ($pH_{final} = 9$–11), removal efficiencies decreased, indicating the interaction mechanism with neutral TMP differed for positively and negatively charged biochar. It has been reported that the carbonyl functional group (C=O) in biochar can be suppressed by the amine (NH_2) from TMP to form C=N while H_2O is released (Putra et al., 2009), and this might be involved in the biosorption process as shown in Fig. 6.

4. Conclusions

The biosorption of pharmaceuticals (DCF and TMP) onto low-cost biosorbents (biochar, wood chippings and macro-algae) at low concentrations was investigated, including consideration of mass transfer, kinetics, isotherms, pH and the mechanisms

involved. Multiple diffusion steps limited mass transfer; biochar was mainly limited by intra-particle diffusion, while macro-algae and wood chippings were mostly controlled by the final adsorptive attachment step. Kinetically, a pseudo-second order model provided the best fit for all systems studied. The equilibrium data for most of the studied systems best fitted the Langmuir model (suggesting a monolayer (chemical) sorption process), while Freundlich offered a good fit for wood chippings and macro-algae (suggesting a multi-layer (physical) sorption). The highest uptake was achieved by biochar for DCF (7.25×10^3 μg g^{-1}), while macro-algae provided better sorption of TMP (7.14×10^4 μg g^{-1}). Both chemical (i.e., electrostatic interactions) and physical (i.e., hydrogen bonding, π-electrons dispersions, etc.) processes were found to be responsible for the biosorption.

These findings highlight the potential to utilize low-cost natural wastes (without additional processing) to remove both negative and positive ionised pharmaceuticals at environmentally relevant, low concentrations. This offers a clean, sustainable and practical water treatment solution for purifying water containing pharmaceutical contaminants, which may have widespread applicability even in rural settings or developing countries.

Declarations of interest

None.

Acknowledgements

This work has been undertaken as part of The Hydro Nation Scholars Programme and supported by The Centre of Expertise for Waters (CREW) on behalf of the Scottish Government. The authors would like to thank the support from the Scottish Government's Rural and Environment Science and Analytical Service Division (RESAS). Also, the authors thank Dr Samia Richards and Dr Luke Beesley (James Hutton Institute) for providing biosorbent materials, Dr Jean Robertson and Angela Main (James Hutton Institute) for supporting FTIR analysis, and Dr Laszlo Csetenyi (University of Dundee) for helping with BET analysis.

Appendix A. Supplementary data

Supplementary data to this article can be found online at https://doi.org/10.1016/j.jclepro.2019.04.081.

References

Adriano, W., Veredas, V., Santana, C., Gonçalves, L.B., 2005. Adsorption of amoxicillin on chitosan beads: kinetics, equilibrium and validation of finite bath models. Biochem. Eng. J. 2, 132–137.
Ali, M.E.M., Abd El-Aty, A.M., Badawy, M.I., Ali, R.K., 2018. Removal of pharmaceutical pollutants from synthetic wastewater using chemically modified biomass of green alga Scenedesmus obliquus. Ecotoxicol. Environ. Saf. 144–152.
Antunes, M., Esteves, V.I., Guégan, R., Crespo, J.S., Fernandes, A.N., Giovanela, M., 2012. Removal of diclofenac sodium from aqueous solution by Isabel grape bagasse. Chem. Eng. J. 114–121.
Artz, R.R.E., Chapman, S.J., Jean Robertson, A.H., Potts, J.M., Laggoun-Défarge, F., Gogo, S., Comont, L., Disnar, J., Francez, A., 2008. FTIR spectroscopy can be used as a screening tool for organic matter quality in regenerating cutover peatlands. Soil Biol. Biochem. 2, 515–527.
Ashton, D., Hilton, M., Thomas, K.V., 2004. Investigating the environmental transport of human pharmaceuticals to streams in the United Kingdom. Sci. Total Environ. 1–3, 167–184.
aus der Beek, T., Weber, F., Bergmann, A., Hickmann, S., Ebert, I., Hein, A., Küster, A., 2016. Pharmaceuticals in the environment—global occurrences and perspectives. Environ. Toxicol. Chem. 4, 823–835.
Baccar, R., Sarrà, M., Bouzid, J., Feki, M., Blánquez, P., 2012. Removal of pharmaceutical compounds by activated carbon prepared from agricultural by-product. Chem. Eng. J. 310–317.
Barbosa, M.O., Moreira, N.F.F., Ribeiro, A.R., Pereira, M.F.R., Silva, A.M.T., 2016. Occurrence and removal of organic micropollutants: an overview of the watch list of EU Decision 2015/495. Water Res. 257–279.
Beesley, L., Marmiroli, M., Pagano, L., Pigoni, V., Fellet, G., Fresno, T., Vamerali, T., Bandiera, M., Marmiroli, N., 2013. Biochar addition to an arsenic contaminated soil increases arsenic concentrations in the pore water but reduces uptake to tomato plants (Solanum lycopersicum L.). Sci. Total Environ. 598–603.
Bhadra, B.N., Ahmed, I., Kim, S., Jhung, S.H., 2017. Adsorptive removal of ibuprofen and diclofenac from water using metal-organic framework-derived porous carbon. Chem. Eng. J. 50–58.
Bhadra, B.N., Seo, P.W., Jhung, S.H., 2016. Adsorption of diclofenac sodium from water using oxidized activated carbon. Chem. Eng. J. 27–34.
Bonvin, F., Jost, L., Randin, L., Bonvin, E., Kohn, T., 2016. Super-fine powdered activated carbon (SPAC) for efficient removal of micropollutants from wastewater treatment plant effluent. Water Res. 90–99.
Bu, Q., Wang, B., Huang, J., Deng, S., Yu, G., 2013. Pharmaceuticals and personal care products in the aquatic environment in China: a review. J. Hazard Mater. 189–211.
Bui, T.X., Choi, H., 2009. Adsorptive removal of selected pharmaceuticals by mesoporous silica SBA-15. J. Hazard Mater. 2, 602–608.
Carlsson, G., Patring, J., Kreuger, J., Norrgren, L., Oskarsson, A., 2013. Toxicity of 15 veterinary pharmaceuticals in zebrafish (Danio rerio) embryos. Aquat. Toxicol. 30–41.
Czech, B., Oleszczuk, P., 2016. Sorption of diclofenac and naproxen onto MWCNT in model wastewater treated by H2O2 and/or UV. Chemosphere 272–278.
De Liguoro, M., Di Leva, V., Dalla Bona, M., Merlanti, R., Caporale, G., Radaelli, G., 2012. Sublethal effects of trimethoprim on four freshwater organisms. Ecotoxicol. Environ. Saf. 114–121.
De Oliveira, T., Guégan, R., Thiebault, T., Le Milbeau, C., Muller, F., Teixeira, V., Giovanela, M., Boussafir, M., 2017. Adsorption of diclofenac onto organoclays: effects of surfactant and environmental (pH and temperature) conditions. J. Hazard Mater. 558–566.
Directive 2015/495, European Commission (EU) Implementing Decision 2015/495 of 20 March 2015 Establishing a Watch List of Substances for Union-wide Monitoring in the Field of Water Policy Pursuant to Directive 2008/105/EC of the European Parliament and of the Council (Notified under Document C(2015) 1756).
Doğan, M., Alkan, M., Onganer, Y., 2000. Adsorption of methylene blue from aqueous solution onto perlite. Water, Air, Soil Pollut. 3, 229–248.
Faria, P.C.C., Órfão, J.J.M., Pereira, M.F.R., 2004. Adsorption of anionic and cationic dyes on activated carbons with different surface chemistries. Water Res. 8, 2043–2052.
Freundlich, H., 1906. Over the adsorption in solution. J. Phys. Chem. 385471, 1100–1107.
Foster, H.R., Burton, G.A., Basu, N., Werner, E.E., 2010. Chronic exposure to fluoxetine (Prozac) causes developmental delays in Rana pipiens larvae. Environ. Toxicol. Chem. 12, 2845–2850.
Hasley, G., 1952. The role of surface heterogeneity. Adv. Catal. 259–267.
Ji, Y., Xie, W., Fan, Y., Shi, Y., Kong, D., Lu, J., 2016. Degradation of trimethoprim by thermo-activated persulfate oxidation: reaction kinetics and transformation mechanisms. Chem. Eng. J. 16–24.
Kasprzyk-Hordern, B., Dinsdale, R.M., Guwy, A.J., 2009. The removal of pharmaceuticals, personal care products, endocrine disruptors and illicit drugs during wastewater treatment and its impact on the quality of receiving waters. Water Res. 2, 363–380.
Kim, S.H., Shon, H.K., Ngo, H.H., 2010. Adsorption characteristics of antibiotics trimethoprim on powdered and granular activated carbon. J. Ind. Eng. Chem. 3, 344–349.
Kuzmanović, M., Ginebreda, A., Petrović, M., Barceló, D., 2015. Risk assessment based prioritization of 200 organic micropollutants in 4 Iberian rivers. Sci. Total Environ. 289–299.
Kyzas, G.Z., Deliyanni, E.A., 2015. Modified activated carbons from potato peels as green environmental-friendly adsorbents for the treatment of pharmaceutical effluents. Chem. Eng. Res. Des. 135–144.
Kyzas, G.Z., Travlou, N.A., Kalogirou, O., Deliyanni, E.A., 2013. Magnetic graphene oxide: effect of preparation route on reactive black 5 adsorption. Materials 4, 1360–1376.
Langmuir, I., 1918. The adsorption of gases on plane surfaces of glass, mica and platinum. J. Am. Chem. Soc. 9, 1361–1403.
Larous, S., Meniai, A., 2016. Adsorption of Diclofenac from aqueous solution using activated carbon prepared from olive stones. Int. J. Hydrogen Energy 24, 10380–10390.
Liu, H., Zhang, J., Bao, N., Cheng, C., Ren, L., Zhang, C., 2012. Textural properties and surface chemistry of lotus stalk-derived activated carbons prepared using different phosphorus oxyacids: adsorption of trimethoprim. J. Hazard Mater. 367–375.
Madikizela, L.M., Chimuka, L., 2016. Synthesis, adsorption and selectivity studies of a polymer imprinted with naproxen, ibuprofen and diclofenac. J. Environ. Chem. Eng. 4, 4029–4037. Part A.
Mailler, R., Gasperi, J., Coquet, Y., Buleté, A., Vulliet, E., Deshayes, S., Zedek, S., Mirande-Bret, C., Eudes, V., Bressy, A., Caupos, E., Moilleron, R., Chebbo, G., Rocher, V., 2016. Removal of a wide range of emerging pollutants from wastewater treatment plant discharges by micro-grain activated carbon in fluidized bed as tertiary treatment at large pilot scale. Sci. Total Environ. 983–996.
Malash, G.F., El-Khaiary, M.I., 2010. Methylene blue adsorption by the waste of Abu-Tartour phosphate rock. J. Colloid Interface Sci. 2, 537–545.
Matias, T., Marques, J., Quina, M.J., Gando-Ferreira, L., Valente, A.J.M., Portugal, A.,

Durães, L., 2015. Silica-based aerogels as adsorbents for phenol-derivative compounds. Colloids Surf. Physicochem. Eng. Aspects 260–269.
Nebot, C., Falcon, R., Boyd, K.G., Gibb, S.W., 2015. Introduction of human pharmaceuticals from wastewater treatment plants into the aquatic environment: a rural perspective. Environ. Sci. Pollut. Control Ser. 14, 10559–10568.
Nielsen, L., Bandosz, T.J., 2016. Analysis of the competitive adsorption of pharmaceuticals on waste derived materials. Chem. Eng. J. 139–147.
Oaks, J.L., Gilbert, M., Virani, M.Z., Watson, R.T., Meteyer, C.U., Rideout, B.A., Shivaprasad, H.L., Ahmed, S., Chaudhry, M.J.I., Arshad, M., Mahmood, S., Ali, A., Khan, A.A., 2004. Diclofenac residues as the cause of vulture population decline in Pakistan. Nature 6975, 630–633.
Pezoti, O., Cazetta, A.L., Souza, I.P.A.F., Bedin, K.C., Martins, A.C., Silva, T.L., Almeida, V.C., 2014. Adsorption studies of methylene blue onto ZnCl2-activated carbon produced from buriti shells (Mauritia flexuosa L.). J. Ind. Eng. Chem. 6, 4401–4407.
Putra, E.K., Pranowo, R., Sunarso, J., Indraswati, N., Ismadji, S., 2009. Performance of activated carbon and bentonite for adsorption of amoxicillin from wastewater: mechanisms, isotherms and kinetics. Water Res. 9, 2419–2430.
Rivera-Utrilla, J., Sánchez-Polo, M., Ferro-García, M.Á., Prados-Joya, G., Ocampo-Pérez, R., 2013. Pharmaceuticals as emerging contaminants and their removal from water. A review. Chemosphere 7, 1268–1287.
Regulation 37/2010, 2010. Council regulation (EU) No 37/2010 of 22 december 2009. Off. J.Eur. Union L15, 1–72.
Sampathkumar, D., Punyamurthy, R., Bennehalli, B., Ranganagowda, R.P., Venkateshappa, S.C., 2014. Natural areca fiber: surface modification and spectral studies. J.: J. Adv. Chem. 10.
Sarmah, A.K., Meyer, M.T., Boxall, A.B.A., 2006. A global perspective on the use, sales, exposure pathways, occurrence, fate and effects of veterinary antibiotics (VAs) in the environment. Chemosphere 5, 725–759.
Shi, K., Wang, X., Guo, Z., Wang, S., Wu, W., 2009. Se(IV) sorption on TiO2: sorption kinetics and surface complexation modeling. Colloid. Surf. Physicochem. Eng. Asp. 1, 90–95.
Sotelo, J.L., Rodríguez, A.R., Mateos, M.M., Hernández, S.D., Torrellas, S.A., Rodríguez, J.G., 2012. Adsorption of pharmaceutical compounds and an endocrine disruptor from aqueous solutions by carbon materials. J. Environ. Sci. Health Part B. 7, 640–652.
Sotelo, J.L., Ovejero, G., Rodríguez, A., Álvarez, S., Galán, J., García, J., 2014. Competitive adsorption studies of caffeine and diclofenac aqueous solutions by activated carbon. Chem. Eng. J. 443–453.
Statista, 2017. https://www.statista.com/statistics/272181/world-pharmaceutical-sales-by-region/.
Suriyanon, N., Punyapalakul, P., Ngamcharussrivichai, C., 2013. Mechanistic study of diclofenac and carbamazepine adsorption on functionalized silica-based porous materials. Chem. Eng. J. 208–218.
Tiwari, D., Lalhriatpuia, C., Lee, S., 2015. Hybrid materials in the removal of diclofenac sodium from aqueous solutions: batch and column studies. J. Ind. Eng. Chem. 167–173.
Vidal, C.B., dos Santos, A.B., do Nascimento, R.F., Bandosz, T.J., 2015. Reactive adsorption of pharmaceuticals on tin oxide pillared montmorillonite: effect of visible light exposure. Chem. Eng. J. 865–875.
Wang, J., Wang, S., 2016. Removal of pharmaceuticals and personal care products (PPCPs) from wastewater: a review. J. Environ. Manag. 620–640.
Weber Jr., W.J., 1984. Evolution of a technology. J. Environ. Eng. 5, 899–917.
Weber, W.J., Morris, J.C., 1963. Kinetics of adsorption on carbon from solution. J. Sanit. Eng. Div. 2, 31–60.
Weigmann, K., 2017. Swimming in a sea of drugs: psychiatric drugs in the aquatic environment could have severe adverse effects on wildlife and ecosystems. EMBO Rep. 10, 1688–1692.
Wilson, B.A., Smith, V.H., deNoyelles, F., Larive, C.K., 2003. Effects of three pharmaceutical and personal care products on natural freshwater algal assemblages. Environ. Sci. Technol. 9, 1713–1719.
Yu, F., Li, Y., Han, S., Ma, J., 2016. Adsorptive removal of antibiotics from aqueous solution using carbon materials. Chemosphere 365–385.
Żółtowska-Aksamitowska, S., Bartczak, P., Zembrzuska, J., Jesionowski, T., 2018. Removal of hazardous non-steroidal anti-inflammatory drugs from aqueous solutions by biosorbent based on chitin and lignin. Sci. Total Environ. 1223–1233.